PIANC De Paepe-Willems Award Winner 2018

SYSTEM OF INSPECTION AND DIAGNOSIS FOR PORT STRUCTURES USING UNMANNED BOAT

KENICHI MIZUNO

Civil Engineer
Works for Penta-Ocean Construction Co, Ltd. in Japan

Keywords: piled piers, inspection, diagnosis, unmanned boat, 3-D modelling
Mots-clés : quais sur pieux, inspection, diagnostic, bateau autonome, modélisation 3D

1. INTRODUCTION

In Japan, the deterioration of port facilities is currently becoming increasingly serious. It is expected that 60 % or more of facilities will be at least 50 years old in 2030. In particular, the upper concrete parts of piled piers are located in the splash zone, showing obvious progress of degradation due to salt damage. Thus, efficient maintenance and control of these facilities are required both now and in the future. However, the investigation of the bottom parts of the superstructures of piled piers that are in service may need to be conducted in peculiar environments, including the presence of moored ships, and the number of engineers available to be assigned to the investigation is insufficient.

Visual inspection of the bottom parts of the superstructures of piled piers in Japan is commonly conducted by a specialist on board a small boat, as shown in Figure 1.1. The specialist ascertains the degree of degradation by visual observation from the boat, fully utilising his knowledge. Inspections frequently overlap with the time when ships are moored or when there is an ebb tide. Sometimes, inspection may be conducted in the night depending on the tide level. Consequently, the inspection needs considerable time and costs. As the person engaged in a prolonged investigation is affected by waves, including wakes during inspection, excessive physical stress is also an issue. In addition, since the boat used in the investigation accommodates two people – the boat operator and the inspector – even a small boat needs a certain size. This prevents the boat from entering narrow areas, such as near the aprons, preventing inspections from being adequately performed. Owing to the long service period of the port facilities, there are cases in which either the maintenance and management data are inappropriately stored or the objective data themselves do not exist, hindering smooth handover of the inspection and diagnostic tasks. Moreover, the judgment of the necessity for repair and selection of a repair method are based on the four-stage standard criteria in Japan (a, b, c, and d), but the results of grading are in most cases biased due to the subjective opinion of the inspectors.

Figure 1.1: Investigation of the undersurface of the superstructure of a piled pier (conventional method)

To resolve these problems, an inspection method using a small unmanned boat with a mounted high-definition camera has been developed to efficiently perform investigation under time and space restrictions without requiring the inspection engineers to physically investigate below piled piers. In addition, a technique of producing 3-D models of target structures from captured images and using them to identify cracks has been developed and a diagnostic method of automatically evaluating the degree of degradation of part members has been established. In this study, these techniques have been applied to 45-year-old piled piers in order to examine the labour-saving characteristics and usefulness of the techniques.

2.   INSPECTION METHOD

To replace the conventional technique of human visual inspection of the bottom parts of the superstructures of piled piers, the technique described herein employs a small unmanned boat with a mounted high-definition camera to perform inspection beneath the superstructure of a piled pier, as shown in Figure 2.1. The particulars of the small boat are described hereafter.
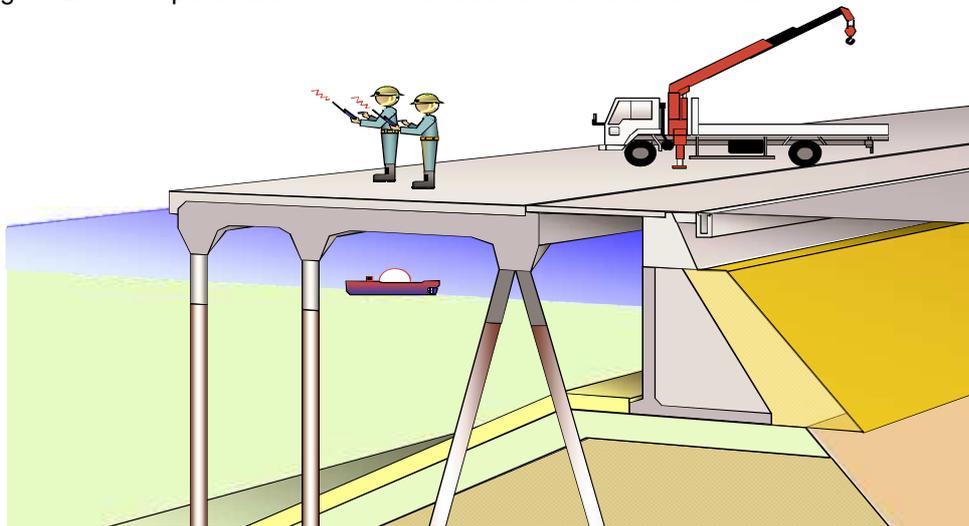
Figure 2.1: Inspection of the undersurface of the superstructure of a piled pier by an unmanned boat

2.1   Small Unmanned Boat

The small unmanned boat selected for this system is produced in the USA and has been previously used in many studies focusing on flow-rate observation and sounding of rivers and the like. Before the devices were mounted, the boat measured 1.8 m long, 0.9 m wide and 0.35 m high and had a mass of approximately 25 kg. The boat has two thrusters at the stern that are powered by batteries stored inside the boat.

To perform an efficient inspection, various devices were installed on the unmanned boat. Figures 2.2 and 2.3 show the unmanned boat before and after mounting the devices, respectively. Upon mounting the devices, the boat became 2.2 m long, 1.1 m wide and 0.65 m high and had a mass of 57.5 kg. It was able to enter below a piled pier as long as the distance between the undersurface of the superstructure of the piled pier and the water surface was approximately 80 cm or more.

Figure 2.2: Unmanned boat (before mounting the devices)
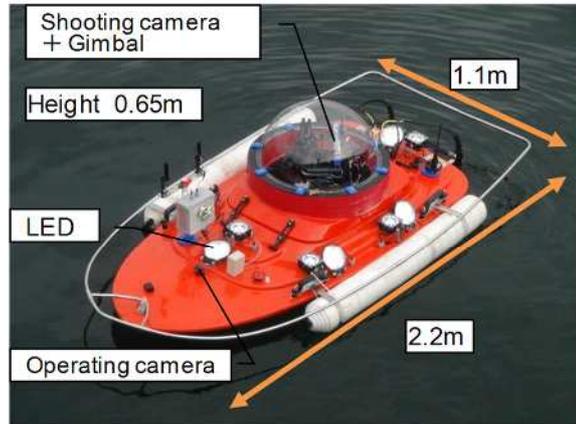
Figure 2.3: Unmanned boat (after mounting the devices)

2.2 Main Components

1) Camera for capturing images
   The image-shooting camera had a maximum resolution of 4,608 × 3,456 pixels (approximately 16 million pixels) for still images and 3,840 × 2,180 pixels (approximately 8.4 million pixels) for video. For example, the camera, equipped with a lens with a focal distance of 7 mm at a distance of 4 m from an object has a resolution of approximately 1.9 mm/pixel when shooting video.

2) Gimbal (a shaking-suppression device)
   At an early stage of development, a camera was directly mounted on a radio-controlled boat, resulting in the captured images being blurry due to the boat's motion under the influence of waves and the inability to focus. To capture stable images using the image-shooting camera, the camera was mounted with the aid of a high-performance three-axis control-type gimbal (shaking-suppression device), which automatically regulates each pitch, roll and yaw motion. This arrangement holds the mounted camera in a particular direction. Figure 2.4 shows a photograph of the gimbal used herein and Figure 2.5 shows a photograph of the gimbal mounted on the boat.

Figure 2.4: Photograph of the gimbal

Figure 2.5: Photograph of the gimbal with image-shooting camera setup

3) Transmitters for camera images

As the image transmission frequency for both the boat operation camera and the image-shooting camera, a high-frequency band was used so that large capacity data, such as images, can be transmitted at a high speed. The transmitter for the images from the boat operation camera was mounted at the bow, protected with a waterproof case. The transmitter for the image-shooting camera was fitted onto the upper part of the gimbal body. Figure 2.6 shows a photograph of the transmitter for the images captured by the boat operation camera. Figure 2.7 shows a photograph of the overall view and installation of the transmitter for the images captured by the image-shooting camera.
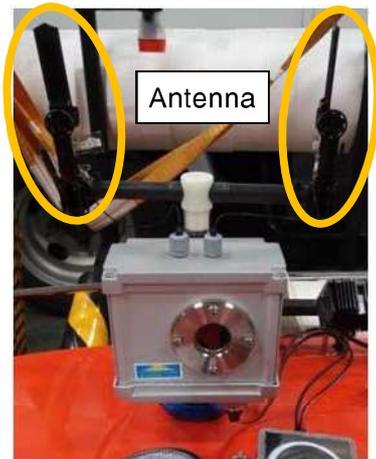
Figure 2.6: Transmitter for the images captured images captured by the boat operation
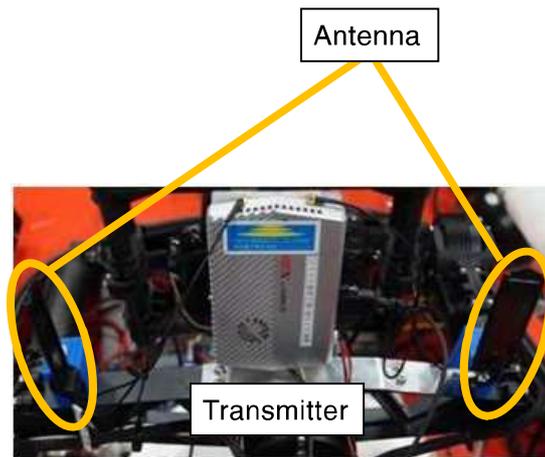
Figure 2.7: Transmitter for the camera by the image-shooting camera

4) Monitor

The images captured by the boat operation and image-shooting cameras are transmitted by their respective transmitters and are received at the monitor placed on the pier, as shown in Figure 2.8. By observing the images on the monitor screen, the boat operator drives the boat and the inspector controls the gimbal. Figure 2.9 shows an image captured by the boat operation camera during an investigation.

Figure 2.8: Image monitor

Figure 2.9: An image captured by the boat operation camera

5) Radio for Boat Operation

a) Normal Radio

The unmanned boat uses a normal radio operating in the 2.4-GHz frequency band. While this frequency band is unsuitable for long-distance communication, its real-time communication capability makes it suitable for boat operation, which relies on the images displayed on the monitor. The transmitter of this radio is placed inside the waterproof case containing the receiver of another

radio for image transmission from the boat operation camera. The transmitter is suspended down from the piled pier to a position that allows communication with the receiver mounted at the boat's bow. Figures 2.10 and 2.11 show the transmitter and receiver of the radio, respectively.
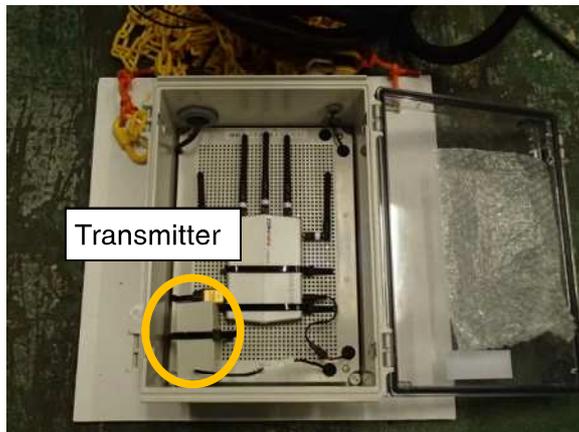
Figure 2.10: Transmitter of the normal radio
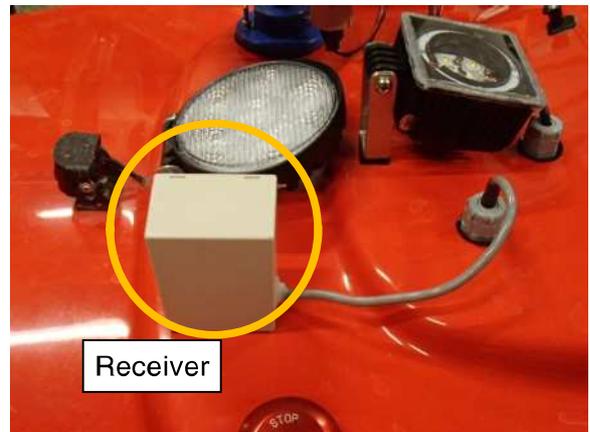
Figure 2.11: Receiver of the normal radio

b) Emergency Radio

In addition to the abovementioned normal radio, the boat operation radio system includes an emergency radio, which uses the 350-MHz frequency band. While the frequency of the emergency radio tends to have a signal lag compared to that of the normal radio, it can be used in emergencies when communication with the normal radio fails during boat operation. Figures 2.12 and 2.13 show the external antennas for the transmitter and receiver of the emergency radio, respectively.

Figure 2.12: Transmission antenna of the emergency radio

Figure 2.13: Reception antenna of the emergency radio

6) LED-Lamp

It is important to have adequate illumination when taking pictures of sufficient quality to capture degradation phenomena, such as cracks, even when sunlight does not regularly reach the undersurface of the superstructure of a piled pier or when ships are moored nearby.

Thus, LED-lamps were installed on the unmanned boat to provide illumination suitable for capturing pictures. Figure 2.14 shows a photograph of the unmanned boat with the LED-lamps illuminated and Figure 2.15 shows a diagrammatic arrangement of the LED-lamps. Each LED-lamp can be turned on and off individually via remote radio operation. This arrangement enabled secure image shooting with illumination, as required for conducting the investigation.

Figure 2.14: LED-lamps when active
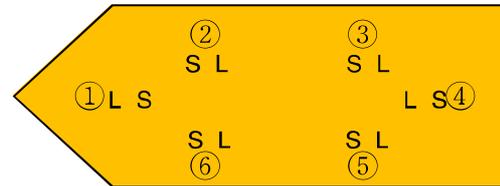
legend
S:small LED lamps
L:large LED lamps

Figure 2.15: Diagrammatic arrangement of LED-lamps

3. DIAGNOSTIC METHOD

3.1 Outline of the Diagnostic Method

A system was developed to automatically diagnose degradation of a structure based on images captured by the image shooting camera installed on the small unmanned boat and centrally manage the maintenance and control data.

At the bottom parts of the superstructure of the piled pier, the position data of the pictured images cannot be obtained due to the unavailability of GNSS. Thus, determining the positions of parts of the structure is impossible. To solve this issue, we initially considered employing a combination of GNSS and an acoustic-positioning system to determine the positions. However, there was a concern that the method might fail due to impediments caused by obstacles such as piles. Consequently, it was decided to perform an analysis based on the Structure-from-Motion-/Multi-View Stereo (SfM/MVS) technique, which automatically estimates the position of a camera and creates 3-D models by image analysis.

Furthermore, the system is configured to automatically diagnose the degree of degradation to evaluate the degradation degree of the entire facility and store the maintenance and control data. To evaluate the degradation degree, first, ortho-images of each part are generated from the created 3-D models. Next, the system is further configured to extract the forms of degradation, such as cracks or exposed reinforcement bars, from the orthochromatic images and the extracted quantitative data are used to automatically evaluate the degree of degradation of each part. A flow-chart of data processing for automatic diagnosis of degradation is shown in Figure 3.1.

Image acquisition with inspection system by radio-controlled boat
Creation of 3-D model with Sf M/MVS analysis
Creation of ortho image for each member from the 3-D model
Registration of facility inspection information and ortho-images in database
Extraction of degraded parts from ortho-images
Automate determination of degree of deterioration of members and facilities

Figure 3.1: Flow-chart of data processing for automatic diagnosis of degradation

3.2 SfM/MVS

SfM/MVS is an image analysis technique that determines the position of a camera and creates 3-D models of structures in a virtual space using a large number of images of the structures captured by the camera at different positions.

The characteristic points are obtained by analysing a plurality of images captured from different positions. Matching those characteristic points between the images creates 3-D models, and further using original images for the texture makes the 3-D models realistic. While conventional photograph-processing requires a great deal of work, such as manually extracting common reference points from the photographed images, the SfM/MVS technique can automatically analyse a large number of images at once and produce 3-D models without requiring high analytical skills. This technique has been spreading in recent years, with representative commercial software, including PhotoScan from Agisoft, Pix4Dmapper from Pix4D, and ContextCapture from Bentley. SfM/MVS has also begun to be adopted for photographic surveys with small unmanned aircraft (commonly referred to as drones – Hayakawa et al., 2016).

Producing 3-D models of the lower part of the superstructure of piled pier by SfM/MVS analysis enables determining the relative positions of cracks or rust stain and obtaining the ortho-images of each part member.

3.3 Automatic Degradation Diagnosis Software

A system was developed to automatically extract and diagnose the degradation of piled piers. The developed software package extracts the degraded parts from the ortho-images created from 3-D models and uses these data to evaluate the degradation degree of each part and the total structure as well as manage the data. Figure 3.2 shows the total system structure. The main functions of the software package are ① registration of 3-D models resulting from the investigation of a piled pier and registration and management of the ortho-images of each part of the structure, ② data processing for identifying the anomalies from the ortho-images of each part of the structure, and ③ output the results, including the expansion plans (DXF format) of the piled pier, which present the identified anomaly conditions. Figure 3.3 shows the main screen of the developed system, which displays the expansion plan of a complete structure, showing all parts together with pictures and the results of the evaluation of degradation degree for each part.

```
①Register data
(1) Name of the project
              Expansion plan view of the piled pier structure
(2) Name of investigation (investigation date)
(3) Name of part member (slab, beam)
              Ortho-image of each part member (2 mm/pixel)
(4) 3-D model
(5) Video of the investigation work
```

```
②Data processing
(1) Extraction to determine crack width and position as well as rust water area
(2) Evaluation of the degradation degree
Automatic evaluation of the degradation degree based on degradation
data and evaluation criteria (part member + entire)
```

```
③Degradation result output
(1) Output DXF of expansion plan and evaluation data
(2) Output report form
```

Figure 3.2: System organisation chart
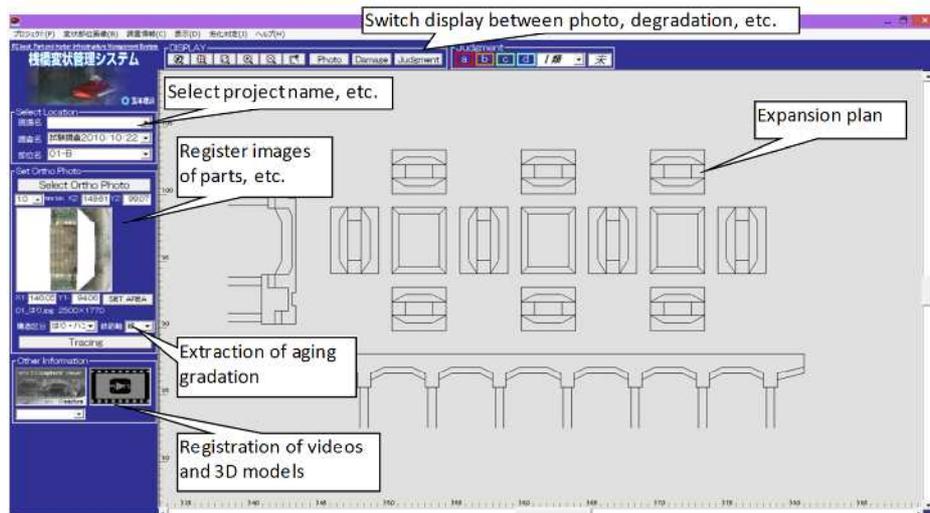
Figure 3.3: Main screen of the developed system

3.4   Extraction of Degradation Information

（1）Method of Extracting Degradation Information

The degradation information that can be determined from photographed images includes cracks, efflorescence, rust stain, exposure of reinforcement, spalling, etc. It is understood that information such as the width, length, and location of cracks and the size of spalling is necessary for objectively grasping the degradation conditions of a structure.

Thus, the extraction of cracks from the images of structures is performed semi-automatically by adopting a method to compute the crack width from the contrast distribution around cracks [Nishimura et al., 2012]. According to this method (Figure 3.4), the crack location is roughly specified by manually drawing a curved line on an image. The width for the analysis (around 20 mm) is given by referring to the curved line, with peaks being automatically located based on the contrast levels in each pixel. Then, the cracks are drawn as a CAD drawing. Semi-automatic extraction is adopted because purely automatic detection of cracks has been shown to suffer issues with accuracy by various institutions. To enable accurate automatic evaluation of the degradation degree, this study uses a semi-automatic extraction method, which can increase the extraction accuracy to a certain extent by allowing the operator to specify the target area. The method of determining crack width involves computation of the crack index (CI) from the distribution of contrast ±4 pixels, as shown in Figure 3.5, and allows crack widths to be obtained from a linear relation (1) between the CI values and crack widths:

$$w = a \times [CI] - b \tag{1}$$

The a and b factors are determined by experience or calibration. The crack width is graded with five levels of colour tone, corresponding to widths of less than 0.5 mm, 0.5 mm to less than 1 mm, 1 mm to less than 2 mm, 2 mm to less than 3 mm, and 3 mm or more. As this method requires a consistent image resolution (2 mm/pixel for this research), lenses are selected to maintain the resolution at 2 mm/pixel or better for each part of the structures during the image-shooting stage. Then, image correction is performed based on the designed drawings when creating ortho-images with a resolution of 2 mm/pixel. Image correction employs bicubic interpolation, which uses 4×4 pixels (16 pixels) around the target point and obtains a final luminance value via cubic interpolation. The extraction of rust stain areas is performed by manually specifying such areas in images and drawing them in CAD.
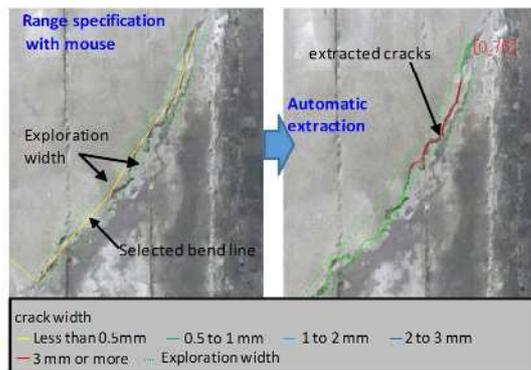
Figure 3.4: Image showing crack identification   Figure 3.5: Crack width calculation method
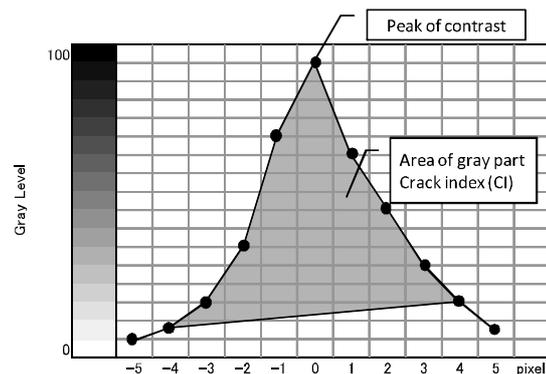
(2) Examination of the Accuracy of Extracting Degradation Information

In terms of detectability of cracks, Koide et al. (1999) reported that the 0.2-mm-wide cracks can be detected in an image with a resolution of approximately 2 mm/pixel. Nishimura et al. (2012) used a method performing semi-automatic crack identification and computation from contrast distribution around cracks, deriving similar results. However, the data obtained by applying SfM/MVS or image correction to the images taken at sea with heavy movements have not been examined. Thus, sheets presenting imitational cracks and rust stain were photographed with the proposed technique at an actual piled pier, and SfM/MVS analysis was applied to the collected images in order to create 3-D models. The widths and lengths of the cracks and the rust stain areas were determined from the orthochromatic images of the 3-D models to examine the accuracy.

There is an existing standard, 'Port Facility Inspection/Diagnosis Guidelines', issued by the Ministry of Land, Infrastructure and Transport (Figure 3.6), applicable to ranking of the degradation conditions of the upper structure of piled piers. This standard is to rate the degradation conditions of the structures into four stages of degradation (a, b, c, and d) mainly based on visual inspection.

(a) Slab

a	Webbed cracks noticed in 50 % or more of the surface area of a part member
	Spalling of cover concrete noticed
	Rust stain noticed in wide areas
b	Webbed cracks noticed in less than 50 % of the surface area of a part member
	Rust stain noticed in some areas
c	Cracks in a single direction or belt-like or efflorescence noticed
	Rust stain noticed in a dotted pattern
d	No anomaly noticed

(b) Beam/haunch

a	Cracks with a width of 3 mm or more noticed along the reinforcement axis
	Spalling of cover concrete noticed
	Rust stain noticed in wide areas
b	Cracks with a width less than 3 mm noticed along the reinforcement axis
	Rust stain noticed in some areas
c	Cracks noticed only in a direction perpendicular to the axis
	Rust stain noted in a dotted pattern
d	No anomaly noticed

Figure 3.6: Degree of degradation evaluation criteria of the upper structure of piled piers
('Port Facility Inspection/Diagnosis Guidelines')

Since the border criterion between the gradation degrees a and b was the existence of a crack that was greater or equal to 3 mm in thickness, the detection of such cracks was examined. The examination involved using sheets on which fake cracks were drawn with lines that were 1, 3 and 5 mm wide and 350 mm long. The accuracy of identifying rust stain areas was examined using sheets (350 mm × 200 mm; area = 700 cm^2) painted black. Figure 3.7 generally shows the sheets imitating the degradation cases. Three sheets each were pasted on the undersurfaces of the beam and a slab of a piled pier, and they were photographed by the image-shooting camera mounted on the unmanned boat.

The speed of the boat at that time was approximately 0.5 m/s, and the photographing period lasted for approximately 15 min. In total, about 800 sheet images (3840 × 2160 pixels) were captured and analysed using SfM/MVS to create 3-D models, which are shown in Figure 3.8. The results of identifying widths and lengths of cracks and rust stain areas are shown in Figures 3.9 and 3.10, respectively. As a result, of the three 5-mm-wide fake cracks, the test measured all of them to be 3 mm wide or more. Of the three 3-mm-wide fake cracks, the test measured two of them as 3 mm wide or more and one of them as 2-3 mm wide. Of the three 1-mm-wide fake cracks, the test measured all of them to be 3 mm wide or less, (of which two cracks to be 1-2 mm wide, one crack to be 0.1-1 mm wide). From these results, it was confirmed that the existence of cracks with a width of 3 mm or more can be identified with an accuracy of 89 % (eight locations out of nine). The difference in the lengths of cracks was 21 mm at the largest. This was assumed to be an error that was attributed to the manual input of the detection area. However, it is considered that in the actual evaluation of the degradation degree, a 20 -mm long crack will not significantly affect the investigation results or the evaluation of the degradation degree. The evaluation of rust stain areas resulted in a maximum difference of approximately 5 %. The cause of the difference is assumed to be due to the errors in SfM/MVS analysis or the errors attributed to the manual input of the detection area. However, it is considered that similarly to the case of crack length detection, the maximum difference of approximately 5 % will not significantly affect the investigation results or the evaluation of the degradation degree.
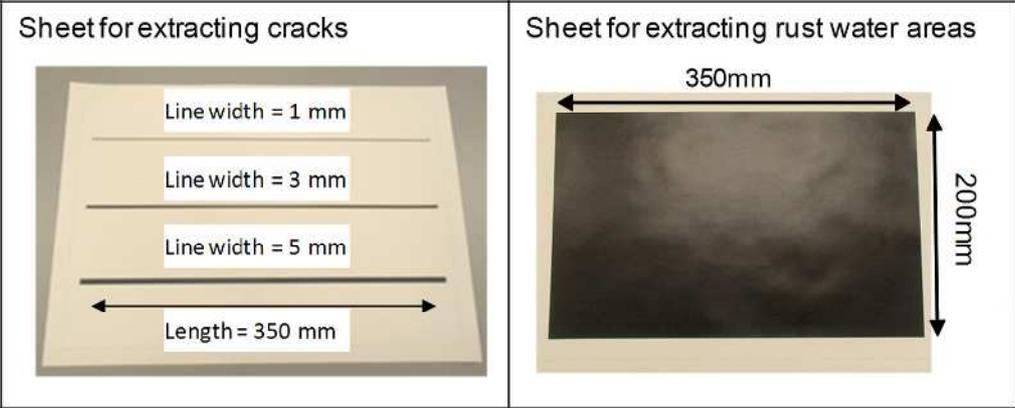
Figure 3.7: Sheets used in the examination
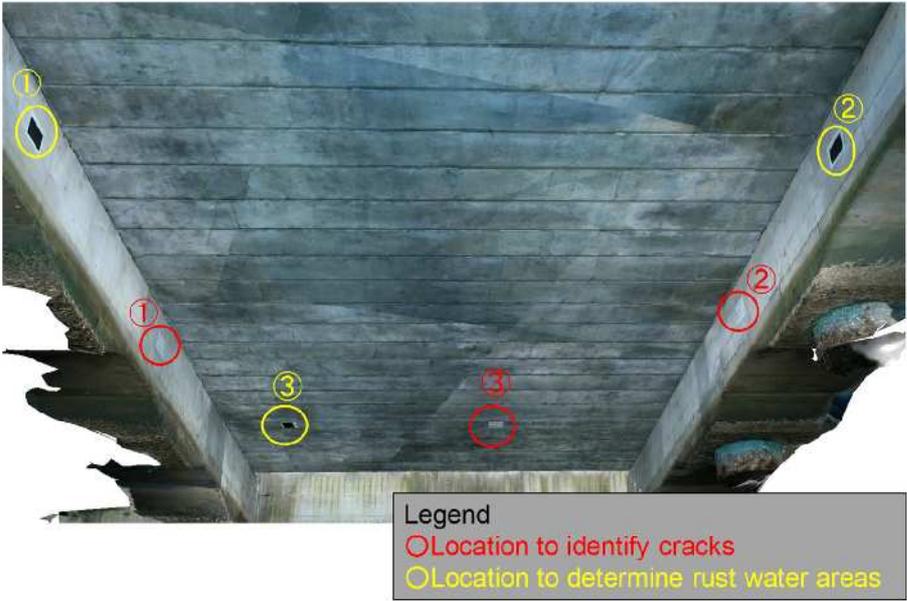
Figure 3.8: 3-D model of the examined piled pier
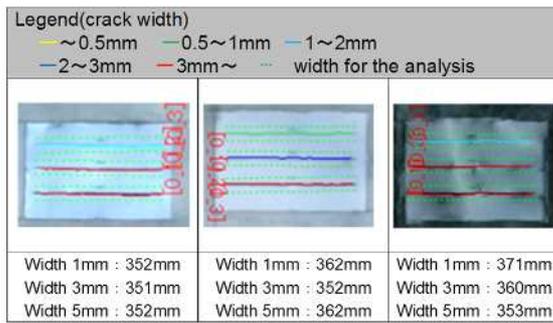
Figure 3.9: Crack evaluation results
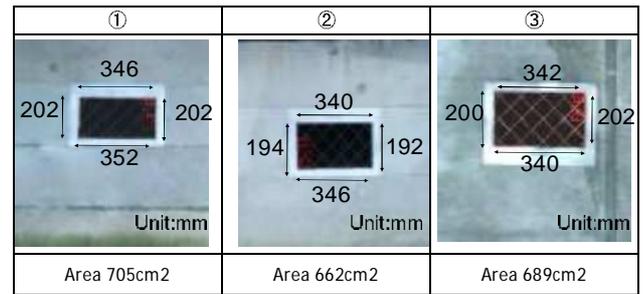
Figure 3.10: Area evaluation results

3.5 Automatic Degradation Diagnosis

This technique is intended to be a method of extracting the degradation information and automatically evaluating the degradation degree based on available data. For this purpose, the standards in 'Port Facility Inspection/Diagnosis Guidelines' were referred to and numerical criteria for each description were established. These criteria are shown in Figure 3.11. The factors for evaluating cracks are their orientation, width and density. Crack density (m/m^2) is defined as crack length (m)/cracked area (m^2). The factor for evaluating the spalling of concrete or exposure of reinforcement is the ratio of degraded parts, which is defined as the area of the degraded parts (m^2)/ the surface area of the member (m^2).

(a) Slab

Port Facility Inspection/Diagnosis Guidelines

a	Webbed cracks noticed in 50 % or more of the surface area of a part member
	Spalling of cover concrete noticed
	Rust stain noticed in wide areas
b	Webbed cracks noticed in less than 50 % of the surface area of a part member
	Rust stain noticed in some areas
c	Cracks in a single direction or belt-like or efflorescence noticed
	Rust stain noticed in a dotted pattern
d	No anomaly noticed

Established evaluation criteria

a	Crack density	2m/m² or more
	Concrete spalling area	1 % or more
	Leaching area of rust stain and exposed rebar area	50 % or more
b	Crack density	1m/m² to 2m/m²
	Leaching area of rust stain and Exposed rebar area	20% to 50%
c	Crack density	1m/m² less than
	Efflorescence area	5 % or more
	Leaching area of rust staint and exposed rebar area	20 % less than
	Other Anomaly	Exist
d	Anomaly	Non-Existant

(b) Beam/Haunch

Port Facility Inspection/Diagnosis Guidelines

a	Cracks with a width of 3 mm or more noticed along the reinforcement axis
	Spalling of cover concrete noticed
	Rust stain noticed in wide areas
b	Cracks with a width less than 3 mm noticed along the reinforcement axis
	Rust stain noticed in some areas
c	Cracks noticed only in a direction perpendicular to the axis
	Rust stain noted in a dotted pattern
d	No anomaly noticed

Established evaluation criteria

a	Crack in the axial direction of the reinforcing bar with a width of 3 mm or more	Exist
	Concrete spalling area	1 % or more
	Leaching area of rust stain and exposed rebar area	50 % or more
b	Crack in the axial direction of the reinforcing bar with a width of 3 mm less than	Exist
	Leaching area of rust stain and Exposed rebar area	20 % to 50 %
c	Crack other than reinforcement axial direction	Exist
	Leaching area of rust stain and Exposed rebar area	20 % less than
	Other Anomaly	Exist
d	Anomaly	Non-Existant

Figure 3.11: Established numerical criteria for the evaluation of the degradation degree

4.   TRIAL TEST AT PILED PIER

To examine the efficiency and usability of this technique, a trial test on an actual piled pier was conducted.

4.1 Outline of the Piled Pier

The plan view and a cross-sectional view of the piled pier on which the trial test was conducted are shown in Figure 4.1. The pier is 80 m long, 20 m wide and 45 years old. The pier has a crane installed on top and is mainly used for unloading materials.

(a) Plan view   (b) Cross-sectional view
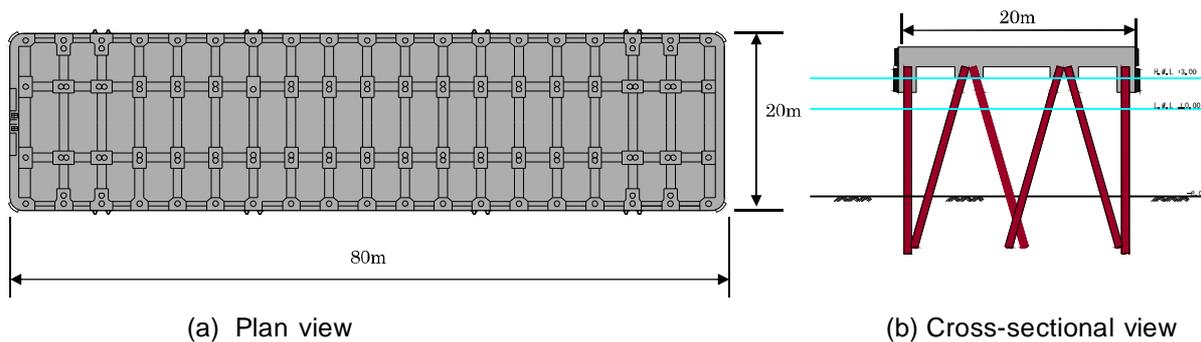
Figure 4.1: Plan view and cross-sectional view of a piled pier

4.2 Trial Test Situation

Figure 4.2 shows scenes from the trial test. The sea showed a significant wave height of about 0.3 m. The distance between the bottom parts of the superstructure of the piled pier and the sea surface was around 0.8-1.5 m. Figure 4.3 shows the position of the radio and the routes through which the unmanned boat travelled. Photographs were captured at least from four angles per point, the examination period of which was 2 h due to the tide conditions. At the slab that required the longest shooting distance, a lens with a focal distance of 7 mm was selected in order to maintain a resolution of 2 mm/pixel or better. The communication with each camera was supposed to be good for the overall length of the pier: 80 m. When the boat was at the farthest from the location of the radio antenna on the pier, i.e. at the pier's diagonal end, radio communication with the monitor occasionally failed temporarily.

(a) Controlling position   (b) Under the superstructure of the piled pier
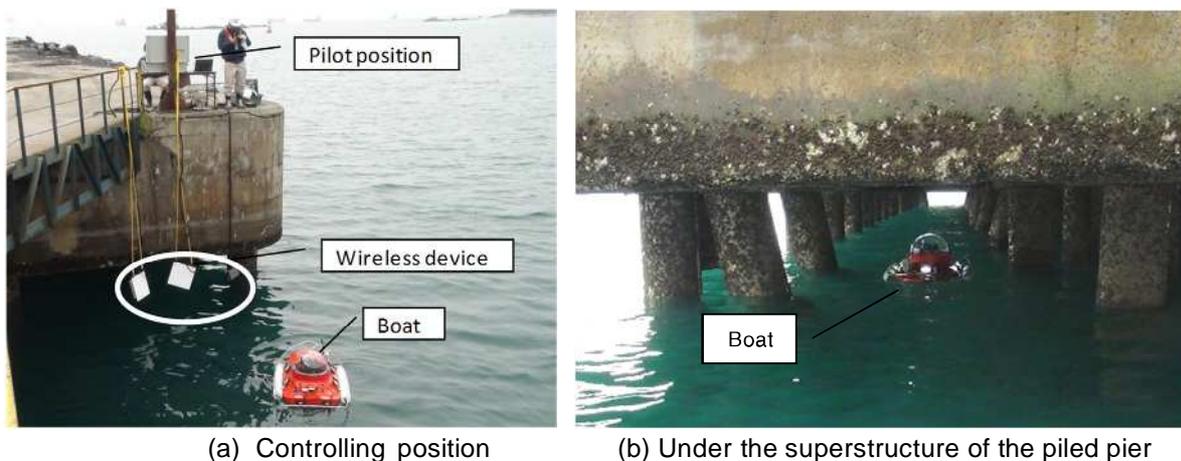
Figure 4.2: Trial test conducted on the undersurface of the superstructure of the piled pier
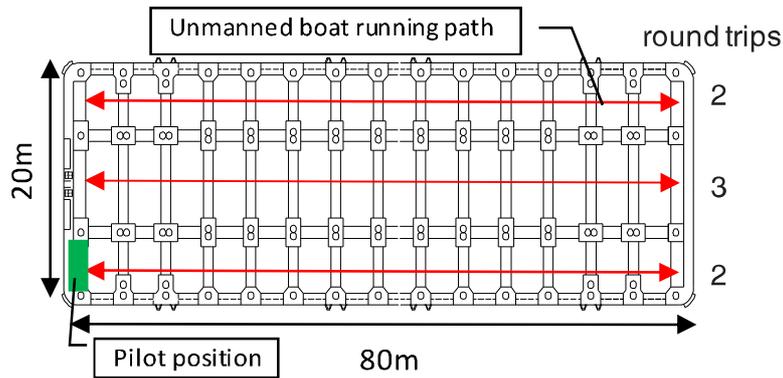
Figure 4.3: Plane of the piled pier

4.3 Result of Trial Test

(1) Examination of Results from Inspection

A 3-D model covering about 1,600 m² of the planar portion of the pier was created using still pictures extracted from 4K (8.29 million pixels) recorded during the trial as shown in Figures 4.4 and 4.5. The 3-D model was created from the images of 2,064 sheets with intervals of about 1 sheet/s using the SfM/MVS software. The 3-D model enabled the determination of the positions of the part members and degradation. The traveling speed of the unmanned boat estimated from the images was about 50 cm/s, from which the overlap rate of the adjacent continuous images along the advancing direction was computed to be about 84 % for slabs.
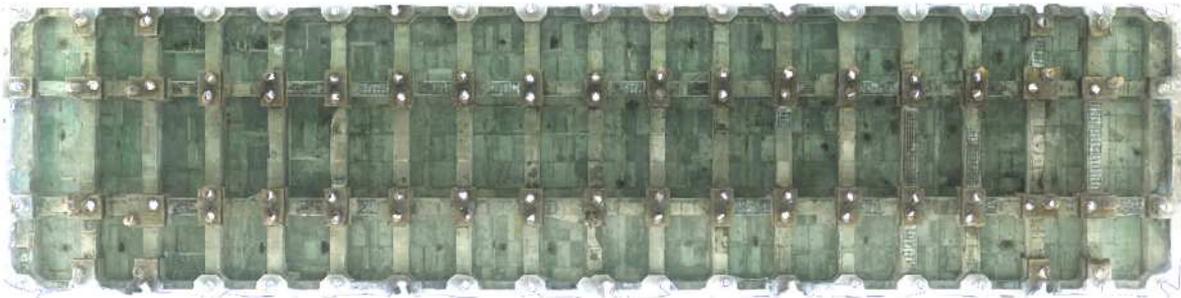
Figure 4.4: 3-D model of the undersurface of the superstructure of the piled pier (far view)

Figure 4.5: 3-D model of the undersurface of the superstructure of the piled pier (close view)

The results from extracting orthochromatic images of each part member from the 3-D model are shown in Figure 4.6. The results were able to show the entire pier as an assembly of expansion plans of each part member. The results of extracting the aging degradation from the orthochromatic images by the technique here are shown in Figure 4.7. In Figures 4.6 and 4.7, on the columns with even numbers, the parts B, D and F are slabs. Examples of an orthochromatic image and the corresponding result of extracting the aging degradation, taken from each beam and slab, are shown in enlarged images and drawings in Figure 4.8. The extraction showed the degradations like spalling of cover concrete, exposure of reinforcement on the bottom face of the beam, cracks, exposing reinforcement bars and efflorescence on the slab. Results from the extraction were used for automatic evaluation of degradation degree.
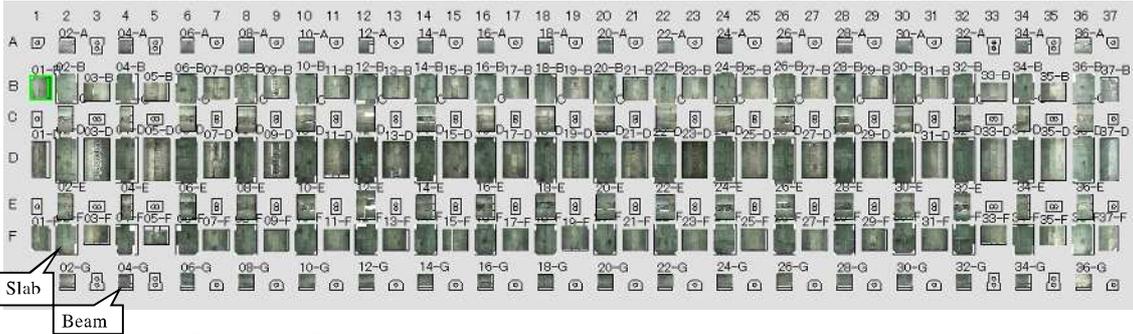
Figure 4.6: Expansion plan of the orthochromatic images of each member
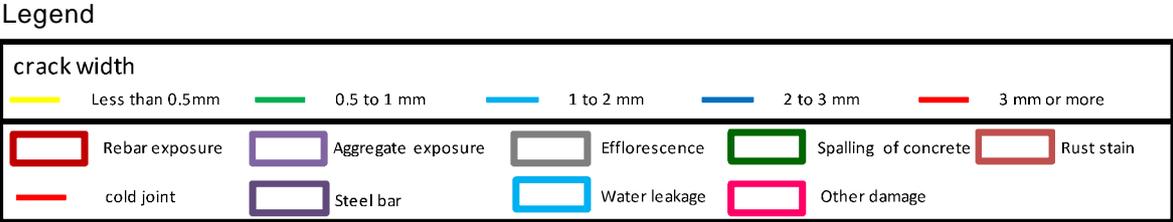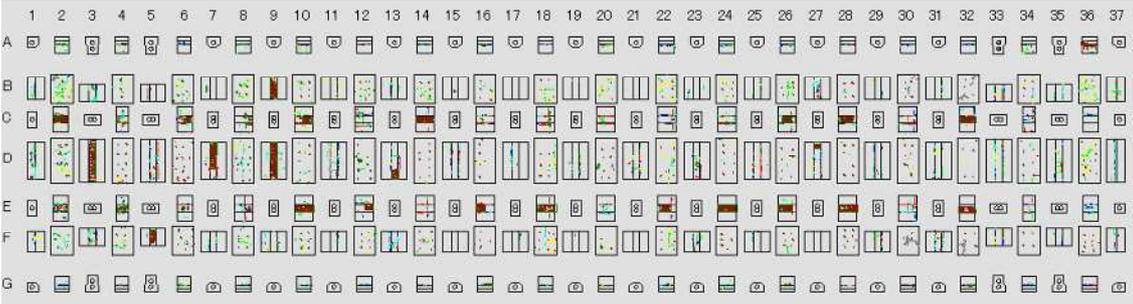
Figure 4.7: Results of extracting aging degradation
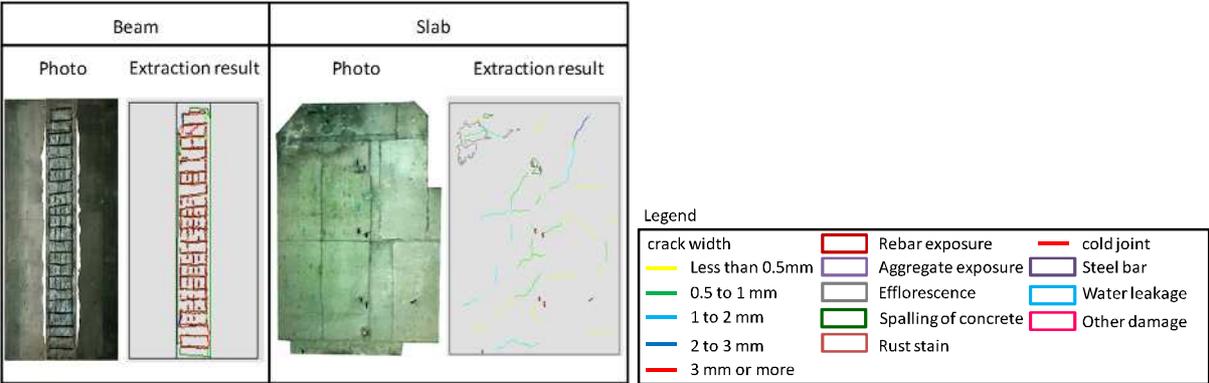
Figure 4.8: Enlarged orthochromatic images and drawings resulting from extracting degradation

At the piled pier where this trial test was conducted, there also had been a human-based visual investigation one year before the investigation by the unmanned boat. The degree of degradation evaluated by the human-based inspection and that evaluated by the method with this technique are compared and shown in Figures 4.9 and 4.10. In Figure 4.9, the encircled letters denote the results from the human-based visual inspection, which differ from those of the method developed here. While results of slabs coincided 100 % (54 members/54 members), results of beams shoed 90 % match (116 members/129 members).

【Slab】
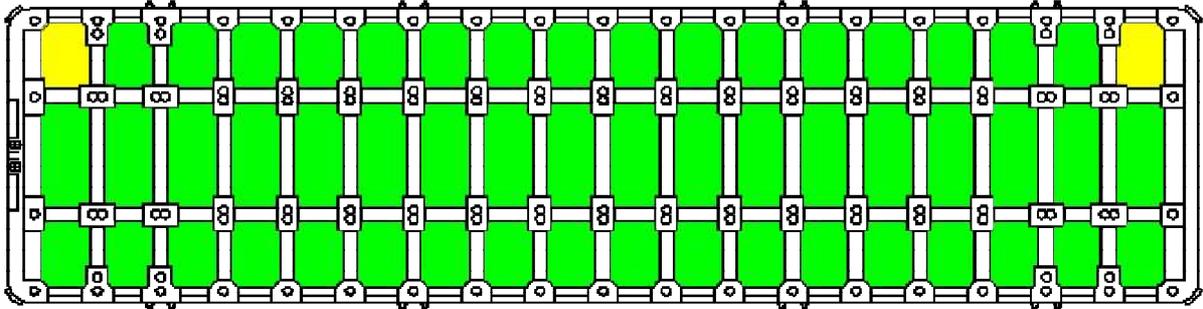
【Beam】
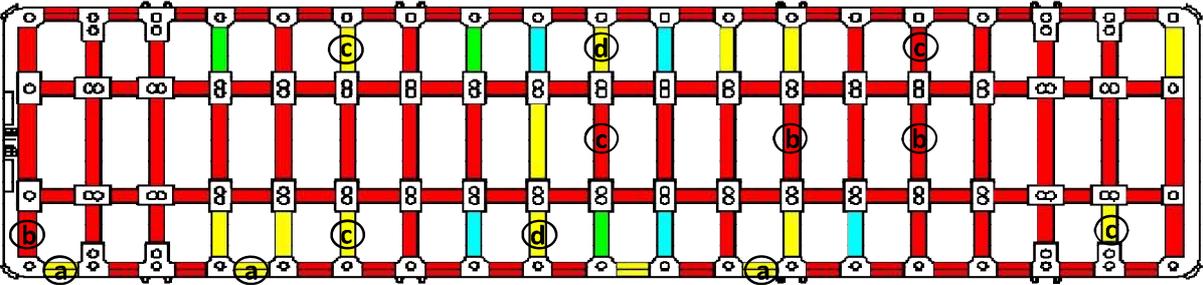
Legend ■ a ■ b ■ c ■ d

○ indicates mismatching. The letters denote evaluations.

Figure 4.9: Comparison of plan views between diagnosis by human inspection and the proposed technique
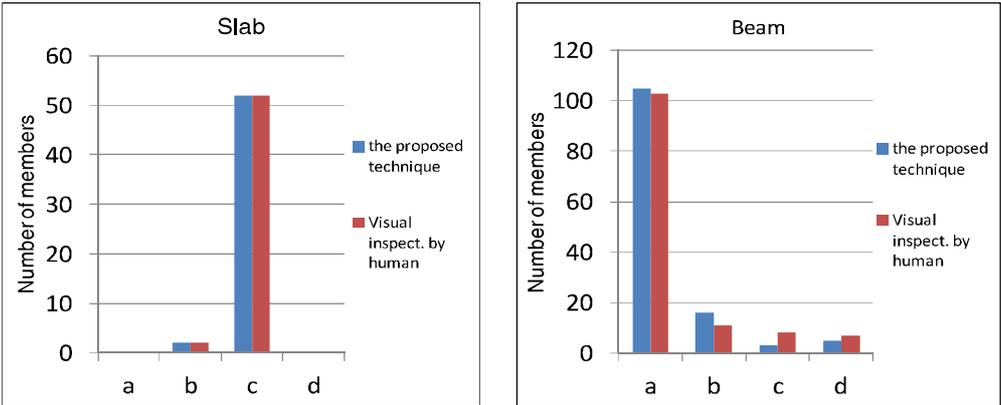
Figure 4.10: Comparison of the distribution of degradation levels obtained by diagnosis by human and the proposed technique

Causes of the difference of 10 % are assumed to be: progress of degradation like spalling, the judgment of putting all the cracks along the axis of reinforcement bars at level b or worse regardless of the length of the cracks, and insufficient extraction of the existence of cracks 3 mm wide or greater. There are 3 locations where extraction of the existence of cracks 3 mm wide or more was insufficient. Their causes

are assumed to be that the width of the particular crack was too large as shown in Figure 4.11 or white blurring which occurred owing to direct light causing the contrast to be lost. Considering that human-based investigation also can be biased depending on subjective view of the inspector, the matching of 90 % seems acceptable.
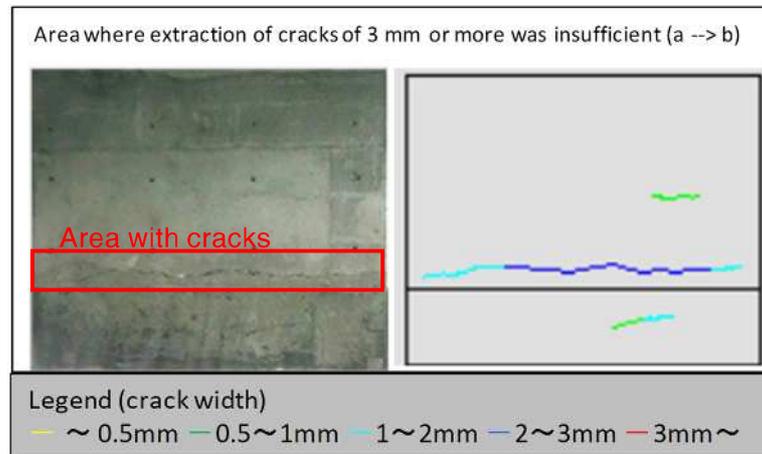
Figure 4.11: An area with different degrees of degradation

(2) Resource Saving Demonstrated by Field Trial Test

The productivity of the human-based standard inspection method in Japan using a small boat was known to be 1,240 m^2/day. With 8 total working hours a day, actual hours available for the investigation would be about 6 hours, excluding preparation and cleaning up. In this trial test, the investigation using the unmanned boat lasted 2 hours and took pictures covering about 1,600 m^2, demonstrating resource saving compared to the standard human-based inspection method in Japan. The maximum investigation time of the unmanned boat is about 4 hours after excluding the time for preparation, battery replacement, and cleaning up. From these results, it is revealed that the expected area of the investigation achievable by the proposed method is about 3,200 m^2/day, i.e. about 2.5 times the efficiency of the standard human-based inspection method in Japan.

5. SUMMARY

The results of this research are summarised below.

We have confirmed that the images of target structures can be captured using an unmanned boat with data transmission systems without requiring a human inspector to enter under the superstructure of the piled pier. This research has developed a method of automatically diagnosing the degradation degree and has enabled the creation of 3-D models of target structures in order to easily detect the degradation conditions. Objective evaluation based on the identified degradation data has been performed using the automatic degradation diagnosis method.

A trial test for the proposed technique was conducted at an actual piled pier. We confirmed that the results of this method matched those of the standard method involving human inspection. Moreover, the proposed method showed an efficiency of about 2.5 times that of the standard method involving human inspection, proving its usability.

6. ACKNOWLEDGEMENT

7. REFERENCES

Hayakawa,Yuichi S. and Obanawa, Hiroyuki (2016): "Aerial Measurements of Topography Using Small UAS and SfM-MVS Photogrammetry", BUTSURI-TANSA, Vol. 69, No.4, pp. 297-309 (in Japanese).

Nishimura, Shozo, Hara, Kenji, Kimoto, Keisuke and Matsuda, Hiroshi (2012): "The Measurement and Draw Damaged Plans at Gunkan-Island by Using 3D Laser Scanner and Digital Camera", Journal of JSPRS, pp.46-53 (in Japanese).

Chun, Pang-jo and Igo, Atsushi (2015): "Crack Detection from Image Using Random Forest", Journal of JSCE, Vol. 71, No.2, pp. I_1-I-8 (in Japanese).

Koide, Hiroshi (1999.10): "A Special Story Study of a Special Purpose Camera", A Monthly journal of medical imaging and information, pp.1-4 (in Japanese).

Ministry of Land Infrastructure and Transport (July 2014): "Port Facility Inspection/Diagnosis Guidelines" (home page), https://www.mlit.go.jp/common/001046912.pdf.

Ministry of Land Infrastructure and Transport (July 2015): "Field Survey Integration Standard for Formulation of Maintenance Plan" (home page), http://www.mlit.go.jp/common/001082501.pdf.

SUMMARY

While port facilities in Japan have long served an important role in the life of the nation, they have issues associated with deterioration, indicating an urgent need to establish and implement efficient and effective maintenance and control methods. In particular, inspections of the bottom parts of the superstructures of piled piers involve work in narrow and dark spaces, reducing their efficiency. Furthermore, in the method of classifying the degradation condition of the piled piers, the degree of degradation of the members is judged by humans based on the four-stage standard criteria in Japan. This poses a problem that the results may be biased depending on the subjective views of the inspectors. To resolve this problem, an inspection method using an unmanned boat with a mounted high-definition camera has been developed. In addition, techniques that enable the production of 3-D models of target structures from pictured images have been developed for extracting and assessing the occurrence of degradation, such as cracks. A technique to automatically evaluate the degree of degradation of part members has been developed. These techniques were applied to the piled pier, for which 45 years had elapsed since their construction, to examine their usefulness and labour-saving ability. As a result, the developed techniques were confirmed to save approximately 2.5 times more local labour than the standard method involving manual inspection, and the results of automatic evaluation of the degree of degradation generally coincided with those of human evaluation.

RESUME

Depuis longtemps, les installations portuaires au Japon jouent un rôle important dans la vie de la nation. Aujourd'hui, elles présentent des détériorations, ce qui indique un besoin urgent d'établir et de mettre en œuvre des méthodes de maintenance et de contrôle efficaces. En particulier, les inspections des parties inférieures des superstructures des quais sur pieu nécessitent des travaux dans des espaces exigus et sombres, ce qui réduit leur efficacité. En outre, la méthode actuelle de classification des pathologies des quais sur pieux et le degré de dégradation des pieux reposent sur une évaluation à dire d'expert, sur la base de la grille standard à quatre niveaux en vigueur au Japon. De ce fait, les résultats peuvent être biaisés en fonction des points de vue subjectifs des inspecteurs. Pour résoudre ce problème, un système d'inspection utilisant un bateau autonome équipé d'une caméra haute définition a été développé. En complément, des méthodes ont été développées pour produire des modèles 3D

des structures à partir des images collectées, afin de visualiser et évaluer l'étendue des dégradations, en particulier les fissures. Une technique d'évaluation automatique du niveau de dégradation des éléments a été mise au point. Cette technique a été expérimentée sur un quai sur pieu construit il y a 45 ans, afin d'évaluer la précision des résultats obtenus et le gain de main-d'œuvre. Cette expérimentation a permis de montrer que les techniques développées réduisent les coûts de main-d'œuvre d'un facteur d'environ 2,5 par rapport à une inspection manuelle, et que les résultats de l'évaluation automatique sont généralement comparables à ceux de l'évaluation humaine.

ZUSAMMENFASSUNG

Obwohl Hafenanlagen in Japan lange eine wichtige Rolle im Leben der Nation gespielt haben, zeigen sie Anzeichen des Verfalls, was darauf hindeutet, dass ein dringender Bedarf besteht, effiziente und effektive Unterhaltungs- und Kontrollmaßnahmen aufzustellen und einzusetzen. Hierbei ist insbesondere die Inspektion der Pfahlgründungen von Anlegestellen hervorzuheben, bei der Arbeiten bei engen und dunklen Verhältnissen durchgeführt werden müssen, was deren Effizienz beeinträchtigt. Darüber hinaus wird die Klassifizierung der Schäden an Teilen der Anlegestellen in Japan anhand von vier Standardkriterien durch Menschen beurteilt. Daraus ergibt sich das Problem, dass die Ergebnisse möglicherweise auf der subjektiven Sichtweise der Inspektoren beruhen. Um dieses Problem zu lösen, wurde eine Inspektionsmethode entwickelt, bei der ein unbemanntes Boot, auf dem eine hochauflösenden Kamera montiert ist, eingesetzt wird. Zusätzlich wurden Techniken entwickelt, die die Erstellung von 3D-Modellen basierend auf Fotos ermöglichen, um Schäden, wie z. B. Risse, festzustellen und zu bewerten. Ein Verfahren zur automatischen Bewertung der Schäden der betroffenen Teile wurde entwickelt. Um den Nutzen und die Möglichkeit der Arbeitseinsparung zu untersuchen, wurden diese Techniken an pfahlgegründeten Anlegestellen, die vor 45 Jahre erbaut wurden, angewandt. Das Ergebnis zeigte, dass durch dieses Verfahren ca. 2,5-mal mehr Arbeit eingespart werden kann wie mit der Standardmethode mittels manueller Inspektion und dass die Ergebnisse der automatischen Bewertung im Allgemeinen mit denen der menschlichen Bewertung übereinstimmen.

RESUMEN

Las instalaciones portuarias en Japón han jugado un papel crucial para el desarrollo del país. Derivado de lo anterior, hay ciertos aspectos relativos a las condiciones de deterioro que soportan que exigen establecer y poner en marcha un programa de inspección y mantenimiento de las mismas. Particularmente en lo que se refiere a operaciones de inspección en las caras inferiores de las superestructuras de muelles de pilotes, dadas las dificultades de acceso que presentan. En el método de clasificación del deterioro de muelles de pilotes en Japón, la identificación de la situación se basa en un criterio de aplicación de cuatro pasos por parte de un inspector. Este hecho plantea el problema de que los resultados están afectados por un factor humano de carácter subjetivo. Para solucionar este problema, se ha desarrollado un sistema de inspección basado en la utilización de embarcaciones no tripuladas sobre las que se montan cámaras de alta definición. Adicionalmente, se han desarrollado técnicas post-proceso de levantamiento 3D de la estructura a partir de las imágenes tomadas, que permiten evaluar las condiciones de degradación mediante la aparición, por ejemplo, de fisuras. Una técnica que permite una evaluación automática de las condiciones de degradación de una parte de la estructura. Este tipo de técnicas se han aplicado a muelles de pilotes construidos hace 45 años, de cara a valorar su utilidad y su capacidad para evitar el uso de mano de obra. Como resultado, este tipo de técnicas han conseguido rebajar en 2,5 veces, aproximadamente, el consumo de mano de obra respecto de los métodos tradicionales, coincidiendo básicamente los resultados de las evaluaciones automáticas con los existentes utilizando el factor humano.